Shallow lakes under alternative states differ in the dominant greenhouse gas emission pathways

Sofia Baliña [ID],[1]* María Laura Sánchez [ID],[1] Irina Izaguirre [ID],[1] Paul A. del Giorgio [ID][2]

[1]Departamento de Ecología, Genética y Evolución, Facultad de Ciencias Exactas y Naturales, Universidad de Buenos Aires. Instituto de Ecología, Genética y Evolución de Buenos Aires (IEGEBA - CONICET/UBA), Ciudad Autónoma de Buenos Aires, Argentina
[2]Département des Sciences Biologiques, Université du Québec à Montréal, Montréal, Québec, Canada

Abstract

Over the past decades, shallow lakes of the Pampean Plain, Argentina, have been shifting from clear vegetated to turbid phytoplanktonic states due to anthropic pressures. It is not clear, though, if this change in state also involves a change in the overall CO_2 and CH_4 balance of these lakes. Therefore, the main objective of this work was to assess potential differences in the C gas (CH_4 and CO_2) balance of shallow lakes under contrasting states—clear vegetated and turbid phytoplanktonic. We sampled two clear and two turbid shallow lakes in the Pampean region along an annual cycle and we measured all of the major C gas emission pathways: diffusive and ebullitive fluxes and also emissions from emergent vegetated habitats. CO_2 and CH_4 diffusive, ebullitive and vegetated habitat fluxes were comparable between states, but they differed in their relative contribution to the C gas balance because of differences in the coverage of the habitats associated to these pathways. Mean annual, area-weighted CO_2 and CH_4 fluxes of clear lakes were 41.9 ± 19.0 and 15.4 ± 18.5 mmol m^{-2} d^{-1}, respectively, and 7.7 ± 7.3 and 17.9 ± 19.8 mmol m^{-2} d^{-1} for CO_2 and CH_4 fluxes, respectively, for turbid lakes. Despite major differences in the relative contribution of the emission pathways between states, there was a remarkable convergence between states in total greenhouse gas emissions when expressed in terms of mean annual CO_2 equivalent greenhouse gas flux.

Shallow lakes have been shown to play a large role within aquatic networks in terms of nutrient processing (Cheng and Basu 2017) and carbon cycling (Downing 2010). This is related to their high surface area: volume ratio, high rates of input of materials from the surrounding watersheds, frequent mixing and strong influence of sediments on water column processes, reasons why they are large contributors to greenhouse gas (GHG) emissions (Holgerson and Raymond 2016). Also, within a given range of trophic status and morphometry, some shallow lakes can shift between two different alternative states: a clear water state, dominated by submerged macrophytes and with low levels of turbidity; and a turbid-water state, dominated by phytoplankton and with higher turbidity (Scheffer et al. 1993). These two contrasting states result in environmental conditions that may in turn affect multiple ecological and biogeochemical processes, including GHG dynamics. The extent to which CO_2 and CH_4 emissions may be affected by these states depends on the interaction of several processes and factors related to organic matter cycling, such as primary production and respiration rates, carbon burial, aerobic and anaerobic metabolism, and the physical effect of submerged macrophytes on the mixing of the water column (Hilt et al. 2017). The net outcome of these interactions has been explored in situ for CO_2 in some lakes, with fewer studies having assessed the impact on CH_4 (Hilt et al. 2017), but the influence of these alternative states on the overall C gas balance of shallow lakes is difficult to predict with our current understanding. Therefore, it is not clear how a change in the state of shallow lakes may modify their C gas balance.

The effect that changes in the alternative states of lakes may have on CO_2 diffusive flux emissions remains uncertain. Lake CO_2 dynamics reflect in part the net balance between primary production and ecosystem respiration, and several authors have reported a negative relation between daytime

CO_2 diffusive flux and the biomass of primary producers in shallow lakes (Xing et al. 2005; Xing et al. 2006; Balmer and Downing 2011; Trolle et al. 2012). However, the type of dominant primary producer—that is, submerged macrophytes or phytoplankton—may lead to different CO_2 dynamics. Some studies have shown higher total productivity in clear macrophyte dominated lakes in comparison with turbid phytoplankton dominated lakes (Kosten et al. 2010; Brothers et al. 2013), which could therefore lead to lower CO_2 diffusive emissions in clear lakes. Yet, in other cases no difference in net ecosystem production between alternative states was found, where differences in primary production across lakes may be driven by total autotrophic biomass rather than by the type of dominant primary producer, suggesting that CO_2 diffusive emissions could be similar between states (Zimmer et al. 2016). Regarding CH_4 dynamics, contrasting results on the effect of alternative states have been also reported in shallow lakes. For example, submerged macrophytes were reported to suppress both diffusive (Davidson et al. 2015) and ebullitive (Davidson et al. 2018) CH_4 fluxes in mesocosm experiments, yet a positive correlation between submerged macrophyte biomass and CH_4 diffusive flux was found in several shallow systems (Xing et al. 2006; Xiao et al. 2017). Similarly, there are reports of no significant effect of phytoplankton biomass on diffusive emissions of CH_4 (Xing et al. 2006; Davidson et al. 2015) and still there are other reports of a positive correlation between diffusive CH_4 emissions and chlorophyll concentrations (Xing et al. 2005; Xiao et al. 2017).

Additionally, and independently of the state, emergent macrophytes (EM) play a significant role in GHG emissions (Bastviken et al. 2004; Desrosiers et al. 2022; Kyzivat et al. 2022). They provide part of the carbon necessary to produce CH_4 in the sediments, but they also transport CH_4 from the sediments to the atmosphere and O_2 from the atmosphere to the sediments, which allows them to survive in anoxic sediments (Chanton 2005). The presence of EM may significantly influence the C balance of shallow lakes and alternative states might strongly influence the relative coverage of EM, since water clarity enhances the coverage of EM (Cheruvelil and Soranno 2008). This interaction between alternative states and EM in shallow lakes adds yet another layer of complexity to the radiative balance—that is, CO_2 equivalent GHG flux between an ecosystem and the atmosphere (Neubauer 2021)—of shallow lakes that needs to be considered.

The Pampean Plain of Argentina, a region with a flat topography, has approximately 146,000 shallow lakes (Geraldi et al. 2011). These lakes existed as a mosaic of clear and turbid alternative states, with bidirectional shifts in their state due to hydrologic or climatic events (Quirós et al. 2006). Intensification of agriculture, use of fertilizer and erosion over the past three decades have led to consistently higher nutrient and sediment loads to these Pampean lakes (Quirós et al. 2006; Vera et al. 2012), which has led in turn to a generalized shift from clear to turbid states observed at a regional scale (Kosten

et al. 2012; Izaguirre et al. 2022). Yet, current understanding does not allow us to predict what this regional change from clear to turbid states may have implied in terms of the overall C gas balance and potential radiative forcing of these lakes, understanding the radiative forcing as an impact on climate change that is generated by a change in the radiative balance of an ecosystem (Neubauer 2021).

Determining the overall C gas balance of shallow lakes requires assessing multiple aspects of GHG dynamics, including dissolved GHG in the water, diffusive fluxes between the water surface and the atmosphere, emergent macrophyte mediated fluxes, as well as methane ebullitive fluxes. In this study we seek to explore the effect of alternative states on GHG dynamics in shallow lakes of the Pampean Plain. Our specific objectives were to study the seasonal dynamics of CO_2 and CH_4 in Pampean shallow lakes under contrasting states, and to estimate their annual C gas balance. In order to accomplish these objectives, we followed seasonal CO_2 and CH_4 surface water concentrations, diffusive water air fluxes, fluxes from emergent vegetation, and CH_4 ebullitive fluxes in two clear vegetated and two turbid phytoplankton shallow lakes located in the Pampean Plain, Argentina.

Methods

Study area

The Pampean Plain (35°32′–36°48′S; 57°47′–58°07′W) is located in the central east region of Argentina. From NE to SW mean annual precipitation range from 1000 to 400 mm, whereas mean annual temperatures vary from 20°C to 14°C from North to South (Diovisalvi et al. 2015). Pampean lakes are shallow (< 3-m mean depth), eutrophic or hypereutrophic, polymictic and are exposed to a high human impact due to the extensive production of cattle and intensive agriculture in the region (Viglizzo et al. 2001).

For this study we selected four shallow lakes of the Pampean Plain (Fig. S1). Two of them are in a turbid phytoplanktonic state (El Burro [BU] and La Salada [SA]), whereas the two other lakes are under a clear vegetated state (La Segunda [SG] and Kakel Huincul [KH], dominated by *Ceratophyllum demersum*). In addition, these four shallow lakes present areas colonized by the emergent macrophyte *Schoenoplectus californicus*.

Sampling design

The four selected shallow lakes were sampled seasonally in the following periods: winter (11–25 June 2018), spring (16–23 October 2019), summer (3–7 February 2019), and autumn (22–30 April 2019). Every lake presents areas covered by EM and areas of open water (OW). To account for this natural heterogeneity, we sampled in OW sites and in EM sites within each shallow lake. To account for the whole water column, we took samples from the sub surface and from near the bottom (within 30 cm of the sediments, using a Niskin horizontal

bottle) in the same site, and we averaged these samples. There- fore, in each lake and in each season, we sampled two sites, OW and EM (including samples from surface and bottom), obtaining four samples per season and per lake. We, therefore, obtained a total of 16 samples for dissolved gas concentrations and other chemical and biological analyses for each lake.

Limnological characterization

At each sampling site we measured several limnological vari- ables including pH and conductivity (HORIBA D 54-E para- metric sensor) and also vertical profiles of temperature and dissolved oxygen (HANNA HI 9146 portable electronic sen- sors). Additionally, we measured air temperature, humidity, atmospheric pressure and wind speed (Kestrel; 4000 Pocket Weather Tracker; Nielsen-Kellerman). In each site we took water samples from sub surface and near bottom to determine turbidity, total phosphorus and total nitrogen (TP and TN, respectively), total suspended solids, dissolved organic carbon (DOC) and dissolved inorganic carbon, colored dissolved organic matter (CDOM), chlorophyll a (Chl a) and the struc- ture of the phytoplankton community. To obtain further insight in the methods used for each determination please refer to the Supporting Information Methods Section S1.

GHG exchanges

GHG exchanges were studied seasonally at each sampling site, analyzing the partial pressure of CH_4 and CO_2 dissolved in water column (pCH_4 and pCO_2), their diffusive and ebullitive fluxes and the fluxes from the vegetated habitat.

Partial pressure of CH_4 and CO_2 in the water

pCH_4 and pCO_2 in water were determined using the head- space technique (Campeau and del Giorgio 2014). Headspace samples were run in a cavity ringdown spectrometer (CRDS; Picarro G2201-i) (Maher et al. 2013) to obtain the concentra- tion and $\delta^{13}C$ isotopic signature of CO_2 and CH_4. The original concentration and $\delta^{13}C$ isotopic signature of CO_2 and CH_4 was then calculated following the equations from Soued and Prairie (2020). Partial pressure (ppmv) was then converted to concentration (μM). For a more detailed description of this method please refer to Supporting Information Methods Section S2.

Chamber flux estimates

Fluxes between the water air interface and fluxes from the EM area were measured using an opaque floating chamber fol- lowing Rasilo et al. (2015). For more information about the chamber see Fig. S2. We took measurements every 5 min for 15 min, obtaining a total of four time points. In each measure- ment, two samples of 30 mL air were taken from inside the chamber and injected into a 30 mL glass pre-evacuated vials equipped with crimped rubber stoppers (Exetainer, Labco) for posterior analysis on a CRDS (Picarro G2201-i). All measure- ments were done between 10:00 h and 16:00 h.

In the EM area, besides measuring the air water diffusive flux, we deployed a chamber above a clump of EM (over mac- rophytes [OM] flux), in order to capture the potential plant- mediated GHG fluxes in addition to the water air diffusive fluxes. In the subsequent sections we refer to the OM flux as vegetated habitat flux, since it includes both plant-mediated flux through the emergent vegetation and also diffusive emis- sions from the water surrounding the vegetation. In this case the chamber was also deployed for 15 min and we took sam- ples every 5 min (for more information see Fig. S2). The diffu- sive flux rates (f_{gas}) were calculated in mmol m^{-2} d^{-1}, following eq. 1 from Supporting Information Methods Section S3.

To obtain further insight on the origin of the GHG released by the EM, we estimated the CO_2 and CH_4 plant-mediated flux by subtracting the diffusive flux (obtained from the chambers deployed over the water in the EM sites, within the vegetation stands) from the OM chambers (Supporting Infor- mation Methods Section S4, eq. 2). We also performed an iso- topic mass balance of the chambers deployed over the water to estimate the isotopic signature of the CO_2 and CH_4 emitted at the water–air interface (Supporting Information Methods Section S4, eq. 3) and also of the OM chambers in order to estimate the isotopic signature of the CO_2 and CH_4 emitted by the plants (Supporting Information Methods Section S4, eq. 4). We then compared these results with the $\delta^{13}C$ isotopic signature of the ambient pCO_2 and pCH_4.

To avoid overestimation of diffusive and emergent macro- phyte CH_4 fluxes, data was checked for CH_4 bubble events: if there was an abrupt increase in CH_4 during the deployment of the chamber or if chamber measurements did not fit to a lin- ear regression, then it was considered an event of ebullition had occurred inside the chamber and the data were discarded. This was not the case for any of the diffusive nor emergent macrophyte CH_4 fluxes measurements.

Ebullitive flux

Methane bubble fluxes were measured using floating inverted funnels (Fig. S6) placed in the water column (DelSontro et al. 2016). In each shallow lake and in each sea- son, six funnels were deployed, three in the EM area and three in the OW area. The duration of the deployment varied according to the season, from 48 h in summer up to 7 d in winter. Upon recovery of the funnels, bubble gas was extracted from the bottle and injected into a 30 mL glass pre- evacuated vials equipped with crimped rubber stoppers (Exetainer; Labco) for later analysis on a CRDS (Picarro G2201-i) in order to determine the concentration of CO_2 and CH_4 in the bubble gas. The remaining water volume in the bottle was measured to derive the volume of gas accumulated during the incubation. The ebullitive flux was calculated in mmol m^{-2} d^{-1}, following eq. 5. Supporting Information Methods Section S5.

In winter, we only captured enough gas to allow gas collection in one funnel, although we were not able to measure GHG concentrations for this gas. We used this value of gas collection and an average of the spring, summer and autumn pCO_2 and pCH_4 in the bubble gas collected to estimate the winter CO_2 and CH_4 ebullitive flux in this funnel. In the remaining winter funnels the gas accumulation was below the threshold that allows collection (approximately 25 mL), and we have assigned this lower threshold of gas accumulation to all of them. To estimate the winter CO_2 and CH_4 ebullitive flux in these funnels we also assigned an average of spring, summer and autumn pCO_2 and pCH_4.

We also used the inverted funnels to capture CH_4 in occluded bubbles released by disturbing the sediments at each lake that were used to derive the source signature of the CH_4. Samples of the released bubbles were analyzed following the same methodology as described above to determine the concentration and $\delta^{13}C$ isotopic signature of CO_2 and CH_4.

Carbon gas balance

To assess the C gas balance of each lake we included diurnal CO_2 and CH_4 diffusive, ebullitive, and emergent vegetated habitat emissions, and also their CO_2 equivalent GHG flux. We first estimated the OW and EM areas in each lake and in each season by means of satellite image analysis. Landsat 8 OLI (L8) images were obtained from the U.S. Geological Survey (https://earthexplorer.usgs.gov/) with a date matching as closely as possible that of the sampling and were processed using ACOLITE (Vanhellemont 2019) software, applying the Floating Algal Index for Turbid Waters algorithm (Dogliotti et al. 2018), to differentiate areas covered by water and by EM. These images were then processed using QGIS software to select the lake area avoiding surrounding land and to quantify the area of EM and OW in each lake and in each season. For a more detailed description of this method please refer to the Supporting Information Methods Section S6.

The C gas balance of each shallow lake was then calculated as the sum of the average annual diffusive, vegetated habitat and ebullitive fluxes, weighted to the proportion of OW area, the proportion of area covered by EM and the proportion of total area, respectively. As these lakes are shallow, we assumed that ebullition occurred throughout the entire surface of the lakes. This accounting process was done separately for CO_2 and CH_4, and also for their sum as CO_2 equivalent GHG fluxes. To calculate the CO_2 equivalent GHG fluxes, CH_4 fluxes were converted considering that CH_4 has a global warming potential of 34 per mass of gas for a time horizon of 100 years (Myhre et al. 2013), and these converted fluxes were added to the measured CO_2 fluxes.

Statistical analysis

To explore differences in pCO_2 or pCH_4 between EM and OW sites, we tested a mixed linear model for clear and turbid lakes and for CO_2 and CH_4, separately. The model included the fixed factors site (EM and OW) and season (winter, spring, summer, and autumn), and the random factor lake (SG, KH, SA, BU). Since there were no significant differences between sites for pCO_2 or pCH_4 for both states, we did not differentiate between the EM and OW sites. To test for seasonal differences in pCO_2 and pCH_4 between states, we applied a mixed linear model with two fixed factors, state and season, and the random factor lake. To test for differences in the annual mean pCO_2 and pCH_4 between states were used a mixed linear model using one fixed factor: state, and two random factors: Shallow Lake and Season. Differences in diffusive, ebullitive and vegetated habitat fluxes between states were also analyzed with a mixed linear model with emission pathway (diffusive, ebullitive, and vegetated habitat) and State as fixed factors, and Lake and Season as random factors. When significant differences were found, we conducted post hoc comparisons.

In all the analyses, data were tested to fit the assumptions of normality and homogeneity of variances. If data did not fit some assumption, we modeled the structure of the variance by adding a function of variance to the already existing model. We tested three different functions (varExp, varPower, varIdent) and chose the one that provided a model with lowest Akaike information criteria (AIC) (Zuur et al. 2009) (Table S1). All tests were performed at the 95% significance level using R version 3.6.2 in the RStudio environment version 1.2.5019 (The R Core Team 2019). Figures were plotted with the R package ggplot2 3.3.2 (Wickham 2016). PCAs were performed using package Vegan 2.5-6 (Oksanen 2019), Mixed Models were tested using package lmerTest 3.1-2 (Kuznetsova et al. 2017) with assumptions being tested using package Car 3.0-8 (Fox and Weisberg 2019). If data did not fit the assumptions, package nlme 3.1-142 (Pinheiro et al. 2019) was used to model heteroscedasticity. To explore post hoc comparisons package emmeans 1.4.8 (Lenth 2020) was used.

Results

Limnological characterization

Clear lakes were characterized by higher average TN, conductivity, and DOC, whereas turbid lakes had higher levels of CDOM, Chl *a*, TP, and turbidity (Fig. S7). For a quantitative description of all the measured variables and of the phytoplankton structure, please refer to Table S2 and Fig. S8, respectively.

CO_2 and CH_4 dissolved in the water column and their fluxes

Given that overall there were no differences in pCO_2 and pCH_4 between OW and EM sites within lakes (Fig. S9), we included all the samples from one lake without differentiating for habitat. We detected changes in pCO_2 and pCH_4 between seasons, including shifts from net sources to net sinks of CO_2. The annual average pCO_2 measured in the air across all sites was 530.7 ± 33.0 ppmv, and average annual pCH_4 air was of

1.7 ± 0.3 ppmv, and these values were used to determine if lakes were under or oversaturated for each GHG. Clear and turbid lakes presented significant differences in pCO_2 depending on the season and state (Season*State $p < 0.05$, df = 3, $F = 14.0$; Fig. 1a). In winter, clear lakes were oversaturated in CO_2 whereas turbid lakes were slightly undersaturated (Tukey test, $p < 0.001$; Fig. 1a). In contrast, in spring clear lakes were undersaturated in CO_2 while turbid lakes were oversaturated (Tukey test, $p < 0.1$). No differences were found between states in summer, when they were undersaturated, nor in autumn, when both states were oversaturated in CO_2. Clear and turbid lakes were always oversaturated with CH_4 but had significant differences depending on the state and the season (Season*State $p < 0.05$, df = 3, $F = 9.9$; Fig. 1c). Turbid lakes had lowest pCH_4 in winter, higher levels in spring, a peak in summer and then a decrease in autumn. Clear lakes had a similar trend, with lowest pCH_4 values in winter, a rise in spring, a marked peak in summer that, unlike turbid lakes, continued high in autumn. No differences in pCH_4 were found between clear and turbid lakes in winter nor in spring. In summer there were no significant differences but clear lakes

presented a higher variability of pCH_4. Lastly, in autumn clear lakes had significant higher levels of pCH_4 compared to turbid lakes (Tukey test, $p < 0.05$).

No differences in the annual average pCO_2 were found between clear and turbid lakes clear (Fig. 1b), but annual average pCH_4 was higher in clear relative to turbid lakes ($p < 0.05$, df = 1, $F = 10.6$; Fig. 1d). Seasonal and annual values of pCO_2 and pCH_4 can be found in Table S3.

Seasonal changes in pCO_2 and pCH_4 were reflected in the diffusive fluxes, with a net influx of CO_2 from the atmosphere when lakes were undersaturated and an efflux of CO_2 when lakes were oversaturated. The seasonal patterns in CO_2 diffusive flux differed between clear and turbid lakes (Fig. 2a,b), as seen for the pCO_2, and this was also reflected in the seasonal predominant metabolism in each state and each season (i.e., autotrophic or heterotrophic, Fig. S10). In winter, clear lakes acted as sources of CO_2 to the atmosphere whereas turbid lakes acted as slight sinks. Clear lakes acted as sinks in spring and summer whereas turbid lakes acted as sources in spring and sinks in summer, coinciding with the shifts in pCO_2 (Fig. 2a). In autumn, both clear and turbid lakes acted
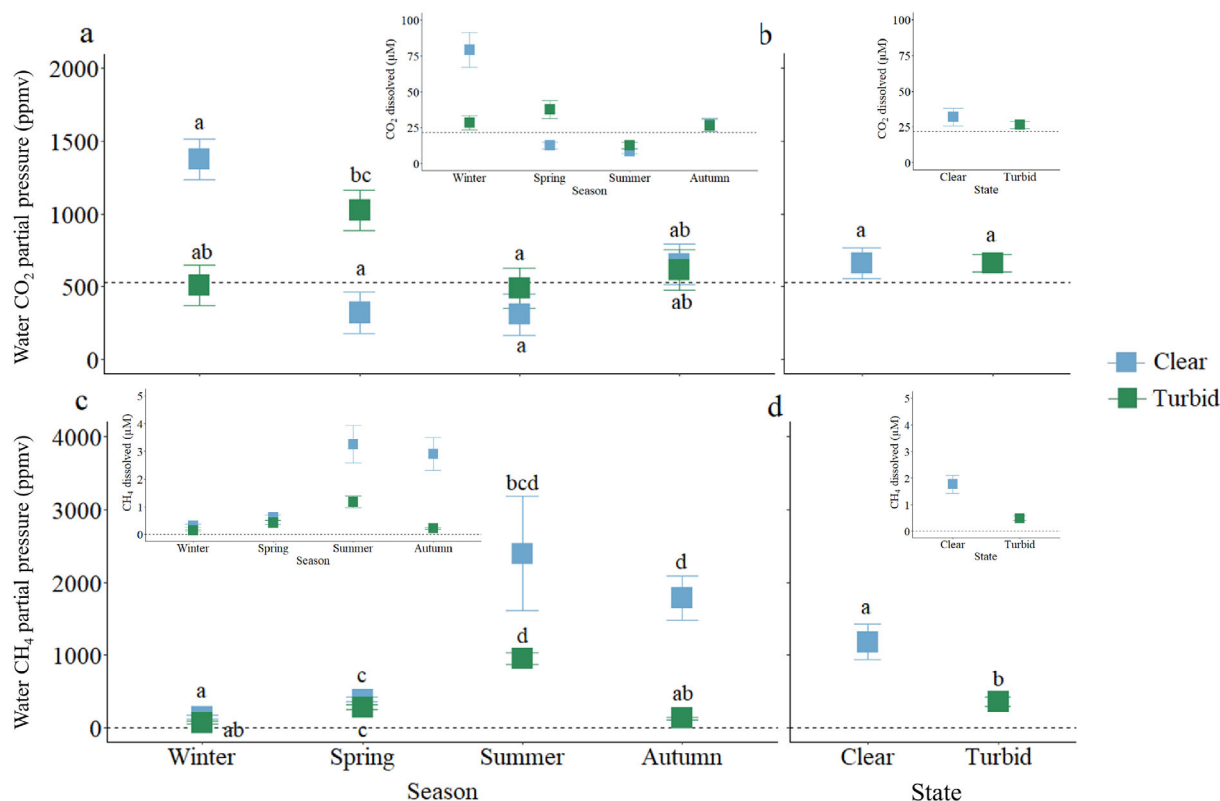

Fig. 1. Seasonal CO_2 (**a**) and CH_4 (**c**) dissolved in the water (ppmv) and annual average CO_2 (**b**) and CH_4 (**d**) dissolved in the water (ppmv), in clear (blue) and turbid (green) shallow lakes. The dotted line in panels **a** and **b** represents the mean atmospheric annual partial pressure of CO_2, and in panels **c** and **d** represents the mean atmospheric annual partial pressure of CH_4. Error bars indicate standard error. Different letters indicate significant differences within each panel. Atmospheric pressure in the Pampean region is very close to 1 atm, which translates into very small differences between ppmv and μatm. Additionally, in each panel we include a smaller figure showing the mean seasonal (**a, c**) and mean annual (**b, d**) concentrations (μM) of CO_2 and CH_4, respectively. The dotted lines in these graphs correspond to the CO_2 and CH_4 concentration in equilibrium with the atmosphere.
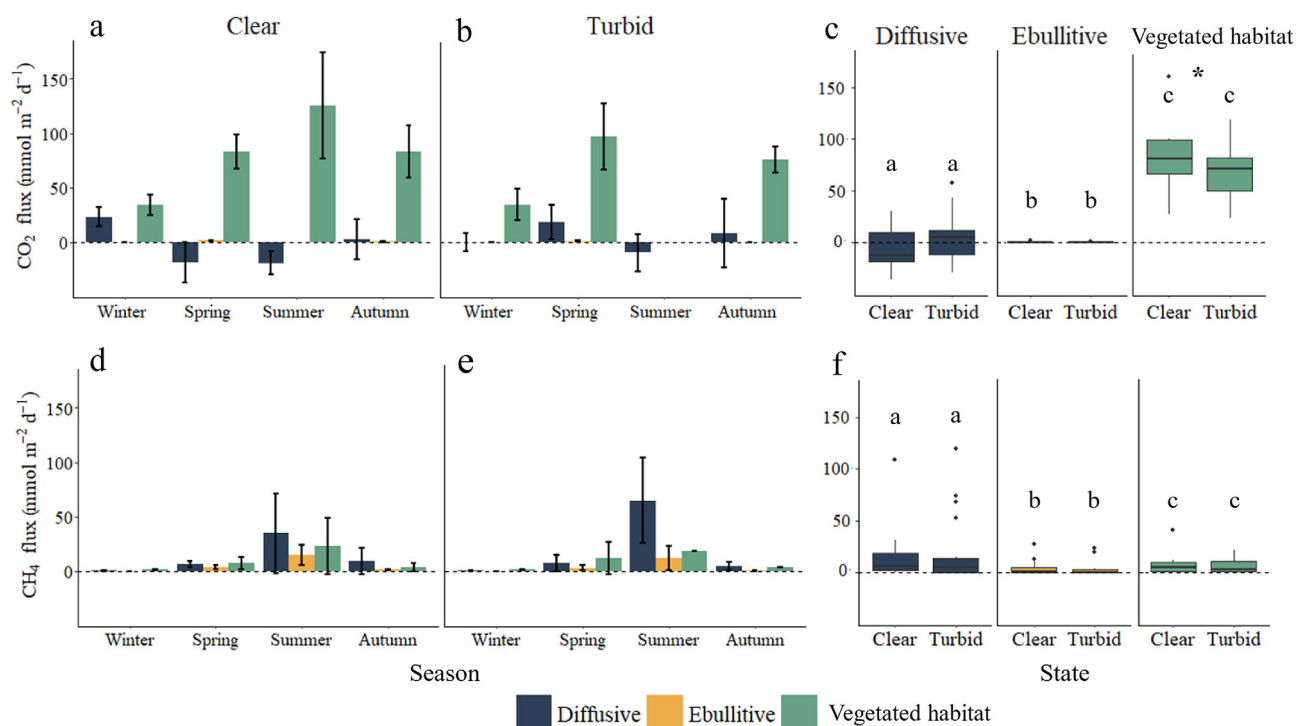
Fig. 2. Seasonal fluxes of CO_2 (**a–c**) and CH_4 (**d–f**) in clear and turbid shallow lakes. Fluxes are divided into diffusive fluxes (blue), ebullitive fluxes (yellow) and fluxes from the vegetated habitat (green). In panels **c** and **f**, different letters indicate significant differences between states for each flux, while the asterisk (*) indicates differences between types of fluxes for each GHG. For turbid lakes in summer no data on the vegetated habitat flux could be collected. Mean ± standard error for each state and each emission pathway in panels **a**, **b**, **d**, and **e** were obtained by averaging all the measurements from the two lakes that corresponded to the same state and emission pathway.

again as sources of CO_2. Regarding CO_2 fluxes in vegetated habitats, clear and turbid lakes presented similar patterns with emission rates that were lower in winter, higher in spring and in summer and then decreasing in autumn. CO_2 ebullitive flux was negligible for both states, accounting for less than 0.5% to the total CO_2 emission.

On an annual basis, there were no significant differences in terms of average CO_2 diffusive, ebullitive or vegetated habitat fluxes between clear and turbid lakes (Fig. 2c), but we found that vegetated habitat fluxes were significantly higher than diffusive and ebullitive fluxes ($p = 0.001$, df = 2, $F = 32.83$; Fig. 2c). Seasonal and annual values of CO_2 diffusive and vegetated habitat fluxes can be found in Table S4. Also, CO_2 diffusive flux of clear lakes had a significant negative linear relation with temperature (Fig. S11a), likely reflecting not a direct temperature effect but rather the negative covariation between macrophyte biomass and temperature along an annual cycle, whereas CO_2 diffusive flux of turbid lakes had no relation with temperature (Fig. S11b). Instead, it had a significant and negative relation with dissolved oxygen and phytoplankton abundance (Fig. S12). Regarding CO_2 flux from vegetated habitats, it presented a significant positive linear relation with temperature, for both clear and turbid lakes (Fig. S11c).

CH_4 diffusive, ebullitive, and vegetated habitat fluxes in clear and turbid lakes had similar seasonal patterns (Fig. 2d,e). All three emission pathways were lower in winter, increased in spring, peaked in summer and then decreased in autumn. On an annual basis, there were no significant differences in all three emission pathways between states, nor between emission pathways, independently of the state (Fig. 2f). Seasonal and annual values of CH_4 diffusive, ebullitive and vegetated habitat fluxes can be found in Table S5. Also, all three CH_4 emission pathways presented a significant and positive relation with temperature (Fig. S11d–f). Our results suggest that EM emitted both CH_4 and CO_2, albeit at very different rates. The resulting CH_4 plant-mediated fluxes varied between -15.6 and 21.4 mmol m^{-2} d^{-1}, with a mean of 2.5 ± 8.7 mmol m^{-2} d^{-1}, whereas the resulting CO_2 plant-mediated fluxes varied between 10.9 and 193.5 mmol m^{-2} d^{-1}, with a mean of 72.8 ± 48.0 mmol m^{-2} d^{-1} (Fig. S3).

Surprisingly, the estimated plant-mediated CO_2 fluxes were much higher than the estimated plant-mediated CH_4 fluxes (Fig. S3). Given that the fluxes from the emergent vegetation were measured in growing plant stands during daytime, we expected to have higher CH_4 emissions and lower CO_2 emissions, but this was not the outcome. To explore this pattern

further, we developed the isotopic mass balance described previously in the method section. The obtained mean isotope ratios of the CO_2 emitted by the EM was -26.5 ± 9.0‰, whereas the mean isotope ratios of the CO_2 emitted by the water and of the CO_2 dissolved in the water were -12.5 ± 2.5‰ and -12.6 ± 4.1‰, respectively (Fig. S4). The obtained mean isotope ratios of the CH_4 released by the EM was -66.3 ± 17.7‰, in the range of the isotope ratios of the fresh sediment CH_4 bubbles (annual means -61.4 ± 1.7‰), but considerably more depleted than the average isotope ratios of CH_4 emitted by the water (-48.6 ± 10.8‰) and of dissolved CH_4 (-40.1 ± 6.0‰; Fig. S5).

Carbon gas balance

On average, clear lakes had fivefold higher total CO_2 emissions than turbid lakes, whereas turbid lakes had 16% higher total CH_4 emissions than clear lakes, leading to a CO_2 equivalent GHG flux similar between states (Table 1). The contribution of the emission pathways to the total CO_2 and CH_4 emissions described in Table 1 differed substantially between states (Fig. 3) due to differences in the relative coverage of the habitats associated to these pathways (Fig. S13; Table S6): CO_2 emissions in clear lakes were largely driven by vegetated habitats (95%), whereas in turbid lakes CO_2 was emitted mainly via OW diffusion (58%) and secondly through vegetated habitats (37%); likewise, CH_4 emissions in clear lakes were for the most part emitted through vegetated habitats (46%) followed by ebullition (32%) and diffusion from OW (22%), whereas in turbid lakes diffusion from OW dominated total CH_4 emissions (76%), followed by ebullition (22%) and lastly by emissions from vegetated habitats (2%). Consequently, the pathways that led to the total CO_2 equivalent GHG fluxes also differed between states: in clear lakes vegetated habitats were the main pathway (55%), followed by ebullition (26%) and diffusion (19%), whereas in turbid lakes diffusion was the main pathway (76%), followed by ebullition (21%), and lastly by emissions from vegetated habitats (3%).

Discussion

The clear and turbid lakes included in this study presented similar characteristics to other clear and turbid shallow lakes from the region, in terms of phytoplankton structure, turbidity, nutrient concentration and dominant primary producers—phytoplankton in turbid lakes and submerged macrophytes in clear lakes (Allende et al. 2009). Therefore, we are confident that the selected lakes are a good representation of the contrasting states that characterize the Pampean Plain.

States had similar annual average pCO_2 but clear lakes had higher annual average pCH_4, implying a differential effect of the state on surface pCO_2 and pCH_4. The similarity in pCO_2 levels suggests a similar net CO_2 metabolism between states. Although we did not measure gross primary production (GPP) or respiration (R) directly, we can estimate the dominant metabolism in each state and in each season by exploring the patterns of CO_2 and O_2 saturation with respect to the atmosphere (Vachon et al. 2020) (Fig. S10). Clear lakes had marked seasonal shifts in net ecosystem metabolism: they were net heterotrophic—that is, R higher than GPP—in winter and autumn and switched to being net autotrophic—that is, GPP higher than R—in spring and summer. Turbid lakes showed a similar seasonal pattern, with relatively limited shifts in net metabolism. These seasonal trends suggest a similar mean annual patterns in net CO_2 metabolism between states and, therefore, could be explaining the similar mean annual surface water pCO_2 between clear and turbid lakes. In this sense, a similar net ecosystem production between a clear and a turbid lake of the Pampean region was also reported by Alfonso et al. (2018), despite major differences in their dominant primary producers.

The contrasting patterns in pCH_4 between states could be due to biological processes, such as a differential CH_4 production or CH_4 oxidation between states (Hilt et al. 2017), or also due to physical processes, such as an effect of the submerged vegetation on the mixing of the water column in clear lakes (Andersen et al. 2017). Submerged macrophytes have a peak of growth in spring and summer that is followed by a decomposition phase that starts in late summer and continues

Table 1. Average area weighted fluxes (mmol m^{-2} d^{-1}). Mean diffusive, ebullitive, and vegetated habitat fluxes weighted for the proportion of the area where each flux occurs. Values for each state and each emission pathway are expressed as the mean of the two lake mean annual area-weighted fluxes ($\pm$ standard deviation for those two values).

Average area weighted fluxes (mmol m^{-2} d^{-1})

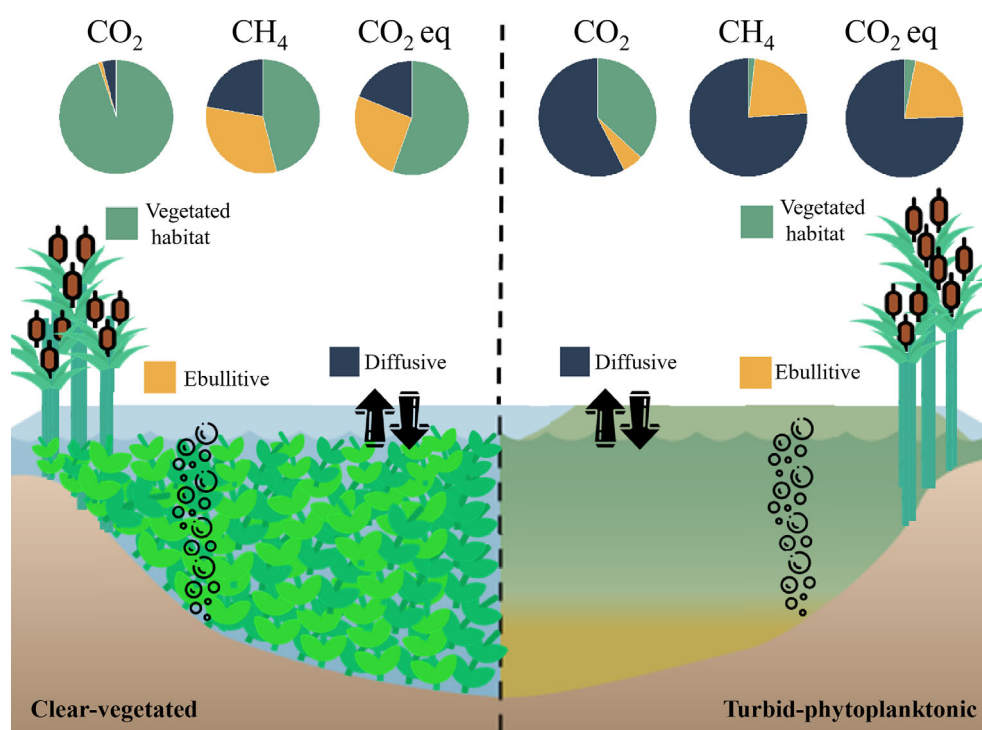|	State	Diffusive	Ebullitive	Vegetated habitat	Total
CO_2	Clear	−1.8 (± 0.6)	0.5 (± 0.2)	43.2 (± 18.1)	41.9 (± 19.0)
	Turbid	4.4 (± 6.8)	0.4 (± 0.0)	2.8 (± 0.4)	7.7 (± 7.3)
CH_4	Clear	3.4 (± 3.1)	4.9 (± 7.3)	7.1 (± 8.1)	15.4 (± 18.5)
	Turbid	13.1 (± 11.7)	4.5 (± 8.0)	0.3 (± 0.0)	17.9 (± 19.8)
CO_2eq	Clear	40.7 (± 39.7)	61.2 (± 90.7)	131.1 (± 117.9)	233.0 (± 248.2)
	Turbid	167.1 (± 152.3)	56.2 (± 99.1)	6.7 (± 0.7)	230.0 (± 252.2)

Fig. 3. Contribution of diffusive (blue), ebullitive (yellow) and vegetated habitat (green) fluxes to the total CO_2, CH_4, and CO_2 equivalent greenhouse gas fluxes for clear (left) and turbid (right) shallow lakes.

during autumn and winter (Best and Meulemans 1979). The peak of pCH_4 in clear lakes was observed in summer and autumn, perhaps associated with decomposition of macrophyte biomass, and it exceeded the peak of turbid lakes. However, diffusive fluxes in these seasons were similar between states. Moreover, mean annual CH_4 exchange velocity from clear lakes was lower than in turbid lakes (Baliña et al. 2022), which could be related to enhanced near-surface turbulence in turbid lakes due to stronger near-surface stratification and greater rates of turbulence dissipation, leading to higher CH_4 exchange velocities (MacIntyre et al. 2021). Similar results were reported by Barbosa et al. (2020), with highest pCH_4 in sites with macrophytes in comparison with OW sites, probably related to macrophyte biomass decomposition, but with similar CH_4 diffusive fluxes between them. At the same time, clear lakes can generate dissolved O_2 supersaturation that could in turn inhibit the activity of methane oxidizing bacteria in the water column (Thottathil et al. 2019), which could contribute to the maintenance of the observed surface water pCH_4.

CH_4 diffusive fluxes in our study ranged between 0.03 mmol m^{-2} d^{-1} in winter and 119.2 mmol m^{-2} d^{-1} in summer, with 85% of the data falling between 0.03 and 25 mmol m^{-2} d^{-1}. A similar range of values was reported for another Pampean shallow lake (Fusé et al. 2016), for an Australian shallow subtropical wetland (Jeffrey et al. 2019*a*), and for boreal ponds (DelSontro et al. 2016). In contrast, lower values

were reported for an Amazon floodplain, including areas of OW, colonized by floating macrophytes and of flooded forest, although there were no differences in CH_4 diffusive flux between habitats (0.04–0.97 mmol m^{-2} d^{-1}, Barbosa et al. 2020). Lower values were also reported for a shallow boreal lake, including areas of OW, submerged and emergent vegetation (0.24–1.1 mmol m^{-2} d^{-1}, Desrosiers et al. 2022), yet much higher values were reported for littoral and pelagic areas of clear and turbid shallow lakes of Uruguay (61.3–270.7 mmol m^{-2} d^{-1}, Colina et al. 2021). CH_4 ebullitive flux ranged from 0.27 mmol m^{-2} d^{-1} in winter up to 27.7 mmol m^{-2} d^{-1} in summer, with an annual mean of 4.7 ± 7.5 mmol m^{-2} d^{-1}. A similar annual mean was found for boreal ponds (4.6 ± 4.1 mmol m^{-2} d^{-1}, DelSontro et al. 2016), for an Australian subtropical wetland (5.5 ± 9.7 mmol m^{-2} d^{-1}; Jeffrey et al. 2019*a*), for the littoral zone of a clear shallow lake and for the pelagic zone of a turbid shallow lake from Uruguay (5.0 ± 0.2 and 3.6 ± 0.2 mmol m^{-2} d^{-1}, respectively; Colina et al. 2021). Yet, a lower mean was reported for a set of Brazilian water bodies (1.1 ± 2.4 mmol m^{-2} d^{-1}; Oliveira Junior et al. 2021), for an Amazon floodplain (1.1 ± 2.6 mmol m^{-2} d^{-1}; Barbosa et al. 2020) and for the unvegetated littoral of a shallow boreal lake (1.84 ± 2.6 mmol m^{-2} d^{-1}, Desrosiers et al. 2022), although Desrosiers et al. (2022) also reported higher means in the areas colonized by the emergent macrophyte *Typha latifolia* and submerged macrophyte *Brasenia schreberi* (6.81 ± 10.8 and 15.9 ± 18.9 mmol m^{-2} d^{-1}, respectively). In our study, clear and

turbid lakes had similar mean annual CH_4 diffusive and ebullitive fluxes despite their contrasting ecological states.

GHG fluxes from the vegetated habitat colonized by the emergent macrophyte *S. californicus* were a major emission pathway. CH_4 fluxes from the vegetated habitats (Table S5), accounted for an average of 33% and 23% of the total CH_4 emitted in clear and turbid lakes, respectively. Areas colonized with *S. californicus* were found to emit on average less CH_4 in a volcanic shallow lake in central America (1.9 mmol m^{-2} d^{-1}; Rejmánková et al. 2018), and vegetated habitats dominated by another species of the same genus (*Scirpus lacustris*) presented lower emissions in small lakes from southern Finland (2.2 and 2.6 mmol m^{-2} d^{-1}; Kankaala et al. 2003, 2005, respectively). Lower fluxes were also reported for areas colonized with other two EM, *Juncus kraussii* and *Phragmites australis*, in an Australian wetland (1.5 and 1.7 mmol m^{-2} d^{-1}, respectively; Jeffrey et al. 2019b). Other studies reported higher fluxes from vegetated habitats of USA wetlands colonized by *Schoenoplectus acutus* (13.1 mmol m^{-2} d^{-1}; Windham-Myers et al. 2018) and by EM of the genera *Typha* (13.7 and 15.2 mmol m^{-2} d^{-1}, Rey-Sanchez et al. 2018, Whiting and Chanton 2001, respectively). These emissions from vegetated habitats combine both diffusive fluxes and plant-mediated emissions, so we estimated the plant-mediated CH_4 fluxes indirectly, by difference from diffusive fluxes (Fig. S3). This same exercise was done by Desrosiers et al. 2022, who reported large plant-mediated CH_4 fluxes that were nevertheless highly dependent on the plant type, with mean emissions from *T. latifolia* being 30.3 ± 30.0 mmol m^{-2} d^{-1} and from *B. schreberi* being 0.62 ± 1.63 mmol m^{-2} d^{-1}. Although our results suggest that EM do emit CH_4, fluxes were relatively low in comparison to the diffusive flux from water within the vegetation stands.

Our results suggest a relevant yet unexpected role of EM in CO_2 emissions, at least for this species or functional macrophyte type and without relativizing the fluxes for the habitat area. We found these plant-mediated CO_2 emissions to be at times high relative to diffusion from surrounding waters, occurring during the daytime and year-round, even when the lake surface was acting as a net sink of CO_2 diffusive flux. Although to our knowledge no diurnal CO_2 emission from EM has been documented to date, we consider that the observation of CO_2 emission by *S. californicus* is plausible and supported by several lines of evidence. In particular, the isotopic mass balance of the CO_2 flux that we captured in the OM chambers required a second source of CO_2 with a stable carbon isotope ratio different from that of the surface water pCO_2. Moreover, the CO_2 flux from the vegetated habitat was significant and positively related with temperature (Fig. S7c), as opposed to the CO_2 diffusive flux in clear and turbid lakes (Fig. S7a,b, respectively), suggesting that this CO_2 flux was controlled by a temperature dependent process, such as heterotrophic microbial metabolism in the sediments. Bridgham and Richardson (1992) reported a seasonal pattern in the CO_2

produced by heterotrophic microbial activity in wetland soils, with highest rates in summer, in coincidence with the patterns of CO_2 emissions from vegetated habitats observed in our study. Heterotrophic microbial activity in the sediments depends on sediment organic matter stocks, presence of electron acceptors—with O_2 being favored—and on TP and DOC loadings, which enhance productivity and organic matter production (D'Angelo and Reddy 1999; Corstanje et al. 2007). As previously described, the Pampean shallow lakes present extremely high TP and DOC levels, and the high productivity of primary producers in each state likely generates large amounts of detrital organic matter in the sediment. In addition, EM can survive in these anaerobic sediments because they transport O_2 from the atmosphere down to their roots (Laanbroek 2010). All of these factors together could generate a scenario that favors high microbial activity in the upper sediments that surround roots of the emergent vegetation. In fact, Faußer et al. 2016 and references therein, have reported accumulation of CO_2 in the aerenchyma of different EM (*P. australis*, *S. lacustris*, *Cyperus papyrus*, *T. latifolia*) which could not be explained by plant aeration and was related to biological processes in the submerged zones, such as aerobic respiration and anaerobic fermentation. Another possible temperature dependent process occurring in these upper sediments could be CH_4 oxidation (Shelley et al. 2015). The fact that the isotopic signature of the CO_2 emitted directly by the EM was in the range of −26.5 ± 9.0‰, which is more negative than the signature of most terrestrial and aquatic carbon sources (Michener and Lajtha 2008), offers indirect evidence that at least a portion of this sediment CO_2 might have originated from CH_4 oxidation. Noyce and Megonigal (2021) reported that *Schoenoplectus* had on average lower CH_4 emissions than *Spartina*, and they linked this to a higher oxidation of the rhizosphere for *Schoenoplectus*, a genera that they denominated net oxidizer of the rhizosphere. Overall, the results reported here underline the relevance of including fluxes from vegetated habitats within C gas balances of shallow water bodies. Furthermore, they highlight the importance of considering CO_2 fluxes mediated by emergent vegetation as a significant emission pathway in shallow systems.

All CO_2 diffusive flux measurements in this study were carried out during the day, but in such productive lakes the nighttime activity may profoundly affect these fluxes and even reverse them. Nighttime emissions were found to exceed daytime CO_2 emissions in several freshwater systems (39% Attermeyer et al. 2021, 27% Gómez-Gener et al. 2021, and 70% Liu et al. 2016). If we apply a nighttime CO_2 correction factor obtained from the studies mentioned above (an average nighttime increase of 54.5 ± 21.9%) to our average area-weighted diurnal CO_2 fluxes (−1.8 ± 0.6 and 4.4 ± 6.8 mmol m^{-2} d^{-1} for clear and turbid lakes, respectively), our average diurnal estimates would be in the order of −1.4 ± 0.7 and 5.4 ± 7.6 mmol m^{-2} d^{-1} for clear and turbid lakes, respectively. Although this is a rough and conservative

approximation, it does provide an idea of the potential magnitude of nighttime effect on CO_2 diffusive fluxes in these shallow lakes.

The contribution of the emission pathways to the C gas balance differed between states: in clear lakes emissions from the vegetated habitat were the dominant pathway due to a higher coverage of emergent vegetation, whereas in turbid lakes diffusion was the main pathway because of a higher relative area of OW. Jeffrey et al. (2019*a*) found that emissions from the emergent vegetated habitat accounted for 59% of the annual CH_4 emissions in an Australian subtropical wetland, followed by diffusion (21%) and ebullition (20%). Kyzivat et al. (2022) also demonstrated the importance of including emergent macrophyte emissions, since accounting for their coverage increased lake CH_4 emission estimates by more than 21% in a subarctic-boreal region. In our study, CH_4 emission from the vegetated habitat was also a very important pathway in clear lakes (accounting for 46% of CH_4 emissions), but not for turbid lakes, where it only accounted for 2% of the emissions. In contrast, CH_4 diffusive evasion accounted for 73% of emissions in turbid lakes. We found that CH_4 ebullition had a similar contribution between states, with 32% and 25% for clear and turbid lakes, respectively. Our results further show that diffusive, ebullitive and vegetated habitat flux rates were comparable between the two states (Fig. 2), but that the two states differed in the relative contribution of these pathways to the total C gas balance, particularly diffusive and vegetated habitat fluxes (Fig. 3) because of differences in the coverage of the respective habitats associated to these pathways (Fig. S13; Table S6). In spite of these fundamental differences in emission pathways and in other functional aspects, the mean annual radiative balance of the two lake states—that is, total C fluxes expressed as CO_2 equivalent GHG flux—was comparable. This is relevant in a broader perspective because it suggests that the shifts from clear to turbid states in Pampean shallow lakes that have been occurring due to climatic and anthropic pressures, may not have fundamentally altered the overall regional radiative forcing, although this point needs to be further explored. Furthermore, our results confirm the major role of emergent vegetation in CH_4 dynamics, but also highlight their dual role in CO_2 fluxes, both as primary producers taking up atmospheric CO_2, as well as major conduits of CO_2 from sediments to the atmosphere.

Data availability statement

The raw data supporting the conclusion of this article will be made available by the authors, without undue reservation.

References

Alfonso, M. B., A. S. Brendel, A. J. Vitale, C. Seitz, M. C. Piccolo, and G. M. Eduardo Perillo. 2018. Drivers of ecosystem metabolism in two managed shallow lakes with different salinity and trophic conditions: The sauce Grande and La Salada Lakes (Argentina). Water **10**: 1136. doi:10.3390/w10091136

Allende, L., G. Tell, H. Zagarese, A. Torremorell, G. Pérez, J. Bustingorry, R. Escaray, and I. Izaguirre. 2009. Phytoplankton and primary production in clear-vegetated, inorganic-turbid, and algal-turbid shallow lakes from the pampa plain (Argentina). Hydrobiologia **624**: 45–60. doi:10.1007/s10750-008-9665-9

Andersen, M. R., T. Kragh, and K. Sand-Jensen. 2017. Extreme diel dissolved oxygen and carbon cycles in shallow vegetated lakes. Proc. R. Soc. B Biol. Sci. **284**: 20171427. doi:10.1098/rspb.2017.1427

Attermeyer, K., and others. 2021. Carbon dioxide fluxes increase from day to night across European streams. Commun. Earth Environ. **2**: 118. doi:10.1038/s43247-021-00192-w

Baliña, S., M. L. Sánchez, and P. A. del Giorgio. 2022. Physical Factors and Microbubble Formation Explain Differences in CH4 Dynamics Between Shallow Lakes Under Alternative States. Front. Environ. Sci. **10**: 1–11. doi:10.3389/fenvs.2022.892339

Balmer, M. B., and J. A. Downing. 2011. Carbon dioxide concentrations in eutrophic lakes: Undersaturation implies atmospheric uptake. Inland Waters **1**: 125–132. doi:10.5268/IW-1.2.366

Barbosa, P. M., J. M. Melack, J. H. F. Amaral, S. MacIntyre, D. Kasper, A. Cortés, V. F. Farjalla, and B. R. Forsberg. 2020. Dissolved methane concentrations and fluxes to the atmosphere from a tropical floodplain lake. Biogeochemistry **148**: 129–151. doi:10.1007/s10533-020-00650-1

Bastviken, D., J. Cole, M. Pace, and L. Tranvik. 2004. Methane emissions from lakes: Dependence of lake characteristics, two regional assessments, and a global estimate. Glob. Biogeochem. Cycles **18**: 1–12. doi:10.1029/2004GB002238

Best, E. P. H., and J. T. Meulemans. 1979. Natural conditions starts in March–June, the potential to grow under experi-physiological activities of these processes were measured in several develop-factors which may influence the carbon fixation rates reported in this paper. Exp. Wer. **6**: 53–65.

Bridgham, S. D., and C. J. Richardson. 1992. Mechanisms controlling (CO_2 and CH_4) in southern peatlands. Soil Biol. Biochem. **24**: 1089–1099. doi:10.1016/0038-0717(92)90058-6

Brothers, S. M., and others. 2013. A regime shift from macrophyte to phytoplankton dominance enhances carbon burial in a shallow, eutrophic lake. Ecosphere **4**: 1–17. doi:10.1890/ES13-00247.1, 10.1890/ES13-00247.1

Campeau, A., and P. A. Del Giorgio. 2014. Patterns in CH_4 and CO_2 concentrations across boreal rivers: Major drivers and implications for fluvial greenhouse emissions under climate change scenarios. Glob. Change Biol. **20**: 1075–1088. doi:10.1111/gcb.12479

Chanton, J. P. 2005. The effect of gas transport on the isotope signature of methane in wetlands. Org. Geochem. **36**: 753–768. doi:10.1016/j.orggeochem.2004.10.007

Cheng, F. Y., and N. B. Basu. 2017. Biogeochemical hotspots: Role of small water bodies in landscape nutrient processing. Water Resour. Res. **53**: 5038–5056. doi:10.1002/2016WR020102

Cheruvelil, K. S., and P. A. Soranno. 2008. Relationships between lake macrophyte cover and lake and landscape features. Aquat. Bot. **88**: 219–227. doi:10.1016/j.aquabot.2007.10.005

Colina, M., S. Kosten, N. Silvera, J. M. Clemente, and M. Meerhoff. 2021. Carbon fluxes in subtropical shallow lakes: Contrasting regimes differ in CH_4 emissions. Hydrobiologia **849**: 3813–3830. doi:10.1007/s10750-021-04752-1

Corstanje, R., K. R. Reddy, J. P. Prenger, S. Newman, and A. V. Ogram. 2007. Soil microbial eco-physiological response to nutrient enrichment in a sub-tropical wetland. Ecol. Indic. **7**: 277–289. doi:10.1016/j.ecolind.2006.02.002

D'Angelo, E. M., and K. R. Reddy. 1999. Regulators of heterotrophic microbial potentials in wetland soils. Soil Biol. Biochem. **31**: 815–830. doi:10.1016/S0038-0717(98)00181-3

Davidson, T. A., J. Audet, J. C. Svenning, T. L. Lauridsen, M. Søndergaard, F. Landkildehus, S. E. Larsen, and E. Jeppesen. 2015. Eutrophication effects on greenhouse gas fluxes from shallow-lake mesocosms override those of climate warming. Glob. Change Biol. **21**: 4449–4463. doi:10.1111/gcb.13062

Davidson, T. A., J. Audet, E. Jeppesen, F. Landkildehus, T. L. Lauridsen, M. Søndergaard, and J. Syväranta. 2018. Synergy between nutrients and warming enhances methane ebullition from experimental lakes. Nat. Clim. Change **8**: 156–160. doi:10.1038/s41558-017-0063-z

DelSontro, T., L. Boutet, A. St-Pierre, P. A. del Giorgio, and Y. T. Prairie. 2016. Methane ebullition and diffusion from northern ponds and lakes regulated by the interaction between temperature and system productivity. Limnol. Oceanogr. **61**: S62–S77. doi:10.1002/lno.10335

Desrosiers, K., T. DelSontro, and P. A. del Giorgio. 2022. Disproportionate contribution of vegetated habitats to the CH_4 and CO_2 budgets of a boreal lake. **25**: 1–20. Ecosystems. doi:10.1007/s10021-021-00730-9

Diovisalvi, N., V. Y. Bohn, M. C. Piccolo, G. M. E. Perillo, C. Baigún, and H. E. Zagarese. 2015. Shallow lakes from the central plains of Argentina: An overview and worldwide comparative analysis of their basic limnological features. Hydrobiologia **752**: 5–20. doi:10.1007/s10750-014-1946-x

Dogliotti, A. I., J. I. Gossn, Q. Vanhellemont, and K. G. Ruddick. 2018. Detecting and quantifying a massive invasion of floating aquatic plants in the Río de la Plata turbid waters using high spatial resolution ocean color imagery. Remote Sens. **10**: 1140. doi:10.3390/rs10071140

Downing, J. A. 2010. Emerging global role of small lakes and ponds: Little things mean a lot. Limnetica **29**: 9–24.

Faußer, A. C., J. Dušek, H. Čížková, and M. Kazda. 2016. Diurnal dynamics of oxygen and carbon dioxide concentrations in shoots and rhizomes of a perennial in a constructed wetland indicate down-regulation of below ground oxygen consumption. AoB Plants **8**: plw025. doi:10.1093/aobpla/plw025

Fox, J., and S. Weisberg. 2019. An R companion to applied regression, 3rd ed. SAGE.

Fusé, V. S., M. E. Priano, K. E. Williams, J. I. Gere, S. A. Guzmán, R. Gratton, and M. P. Juliarena. 2016. Temporal variation in methane emissions in a shallow lake at a southern mid latitude during high and low rainfall periods. Environ. Monit. Assess. **188**: 590. doi:10.1007/s10661-016-5601-z

Geraldi, M. Alejandra, C. Piccolo Maria, and G. E. Perillo. 2011. Lagunas bonaerenses en el paisaje. Cienc. Hoy **21**: 16–22.

Gómez-Gener, L., G. Rocher-Ros, T. Battin, and others. 2021. Global carbon dioxide efflux from rivers enhanced by high nocturnal emissions. Nat. Geosci. **14**: 289–294. doi:10.1038/s41561-021-00722-3

Hilt, S., S. Brothers, E. Jeppesen, A. J. Veraart, and S. Kosten. 2017. Translating regime shifts in shallow lakes into changes in ecosystem functions and services. Bioscience **67**: 928–936. doi:10.1093/biosci/bix106

Holgerson, M. A., and P. A. Raymond. 2016. Large contribution to inland water CO_2 and CH_4 emissions from very small ponds. Nat. Geosci. **9**: 222–226. doi:10.1038/ngeo2654

Izaguirre, I., H. Zagarese, and I. O'Farrell. 2022. The limnological trace of contemporaneous anthropogenic activities in the Pampa Region. Ecol. Austral **32**: 650–662. doi:10.25260/EA.22.32.2.1.1884

Jeffrey, L. C., D. T. Maher, S. G. Johnston, B. P. Kelaher, A. Steven, and D. R. Tait. 2019*a*. Wetland methane emissions dominated by plant-mediated fluxes: Contrasting emissions pathways and seasons within a shallow freshwater subtropical wetland. Limnol. Oceanogr. **64**: 1895–1912. doi:10.1002/lno.11158

Jeffrey, L. C., D. T. Maher, S. G. Johnston, K. Maguire, A. D. L. Steven, and D. R. Tait. 2019*b*. Rhizosphere to the atmosphere: Contrasting methane pathways, fluxes, and geochemical drivers across the terrestrial-aquatic wetland boundary. Biogeosciences **16**: 1799–1815. doi:10.5194/bg-16-1799-2019

Kankaala, P., and others. 2003. Midsummer spatial variation in methane efflux from stands of littoral vegetation in a boreal meso-eutrophic lake. Freshw. Biol. **48**: 1617–1629. doi:10.1046/j.1365-2427.2003.01113.x

Kankaala, P., T. Käki, S. Mäkelä, A. Ojala, H. Pajunen, and L. Arvola. 2005. Methane efflux in relation to plant biomass and sediment characteristics in stands of three common emergent macrophytes in boreal mesoeutrophic lakes. Glob. Chang. Biol. **11**: 145–153. doi:10.1111/j.1365-2486.2004.00888.x

Kosten, S., F. Roland, D. M. L. Da Motta Marques, E. H. Van Nes, N. Mazzeo, L. D. S. L. Sternberg, M. Scheffer, and J. J. Cole. 2010. Climate-dependent CO_2 emissions from lakes. Glob. Biogeochem. Cycles **24**: 1–7. doi:10.1029/2009GB003618

Kosten, S., M. Vernooij, E. H. van Nes, M. de los Á. G. Sagrario, J. G. P. W. Clevers, and M. Scheffer. 2012. Bimodal transparency as an indicator for alternative states in south American lakes. Freshw. Biol. **57**: 1191–1201. doi:10.1111/j.1365-2427.2012.02785.x

Kuznetsova, A., P. B. Brockhoff, and R. H. B. andlenth Christensen. 2017. lmerTest package: Tests in linear mixed effects models. J. Stat. Softw. **82**: 1–26. doi:10.18637/jss.v082.i13

Kyzivat, E. D., and others. 2022. The importance of Lake emergent aquatic vegetation for estimating Arctic-boreal methane emissions. J. Geophys. Res.: Biogeosci. **127**: e2021JG006635. doi:10.1029/2021JG006635

Laanbroek, H. J. 2010. Methane emission from natural wetlands: Interplay between emergent macrophytes and soil microbial processes. A mini-review. Ann. Bot. **105**: 141–153. doi:10.1093/aob/mcp201

Lenth, R. 2020. emmeans: Estimated Marginal Means, aka Least-Squares Means. R package version 1.4.8. Available from https://cran.r-project.org/web/packages/emmeans/index.html

MacIntyre, S., J. H. F. Amaral, and J. M. Melack. 2021. Enhanced turbulence in the upper mixed layer under light winds and heating: Implications for gas fluxes. J. Geophys. Res.: Oceans **126**: e2020JC017026. doi:10.1029/2020JC017026

Maher, D. T., I. R. Santos, J. R. F. W. Leuven, J. M. Oakes, D. V. Erler, M. C. Carvalho, and B. D. Eyre. 2013. Novel use of cavity ring-down spectroscopy to investigate aquatic carbon cycling from microbial to ecosystem scales. Environ. Sci. Technol. **47**: 12938–12945. doi:10.1021/es4027776

Michener, R., and K. Lajtha. 2008. Stable isotopes in ecology and environmental science. John Wiley & Sons.

Myhre, G., and others. 2013. Anthropogenic and natural radiative forcing, p. 659–740. *In* T. F. Stocker and others [eds.], Climate Change 2013: The physical science basis. Contribution of working group I to the Fifth Assessment Report of the intergovernmental panel on climate change. Cambridge University Press. Available from https://www.ipcc.ch/site/assets/uploads/2018/02/WG1AR5_Chapter08_FINAL.pdf

Neubauer, S. C. 2021. Global warming potential is not an ecosystem property. Ecosystems **24**: 2079–2089. doi:10.1007/s10021-021-00631-x

Noyce, G. L., and J. Patrick Megonigal. 2021. Biogeochemical and plant trait mechanisms drive enhanced methane emissions in response to whole-ecosystem warming. Biogeosciences **18**: 2449–2463. doi:10.5194/bg-18-2449-2021

Oksanen, J. F., and others. 2019. vegan: Community Ecology Package. R package version 2.5-6. Available from https://CRAN.R-project.org/package=vegan

Oliveira Junior, E. S., and others. 2021. Water Hyacinth's effect on greenhouse gas fluxes: A field study in a wide variety of tropical water bodies. Ecosystems **24**: 988–1004. doi:10.1007/s10021-020-00564-x

Pinheiro, J., Bates, D., DebRoy, S., Sarkar, D., and R Core Team. 2019. nlme: Linear and Nonlinear Mixed Effects Models. R package version 3.1 142. Available from https://cran.rproject.org/web/packages/nlme/index.html

Quirós, R., Boveri, M. B., Petracchi, C. A., Rennella, A. M., Rosso, J. J., Sosnovsky, A., and von Bernard, H. T. 2006. The effects of the Pampa wetlands agriculturization on shallow lakes eutrophication. Eutrofização na América do Sul: Causas, conseqüências e tecnologias de gestão. São Carlos, Rede EUTROSUL, PROSUL, 1–16.

Rasilo, T., Y. T. Prairie, and P. A. del Giorgio. 2015. Large-scale patterns in summer diffusive CH_4 fluxes across boreal lakes, and contribution to diffusive C emissions. Glob. Change Biol. **21**: 1124–1139. doi:10.1111/gcb.12741

Rejmánková, E., B. W. Sullivan, J. R. Ortiz Aldana, J. M. Snyder, S. T. Castle, and F. Reyes Morales. 2018. Regime shift in the littoral ecosystem of volcanic Lake Atitlán in Central America: Combined role of stochastic event and invasive plant species. Freshw. Biol. **63**: 1088–1106. doi:10.1111/fwb.13119

Rey-Sanchez, A. C., T. H. Morin, K. C. Stefanik, K. Wrighton, and G. Bohrer. 2018. Determining total emissions and environmental drivers of methane flux in a Lake Erie estuarine marsh. Ecol. Eng. **114**: 7–15. doi:10.1016/j.ecoleng.2017.06.042

Scheffer, M., S. H. Hosper, M. L. Meijer, B. Moss, and E. Jeppesen. 1993. Alternative equilibria in shallow lakes. Trends Ecol. Evol. **8**: 275–279. doi:10.1016/0169-5347(93)90254-M

Shelley, F., F. Abdullahi, J. Grey, and M. Trimmer. 2015. Microbial methane cycling in the bed of a chalk river: Oxidation has the potential to match methanogenesis enhanced by warming. Freshw. Biol. **60**: 150–160. doi:10.1111/fwb.12480

Soued, C., and Y. T. Prairie. 2020. The carbon footprint of a Malaysian tropical reservoir: Measured versus modelled estimates highlight the underestimated key role of downstream processes. Biogeosciences **17**: 515–527. doi:10.5194/bg-17-515-2020

The R Core Team. 2019. R: A language and environment for statistical computing. R Foundation for Statistical Computing. Available from https://www.r-project.org/

Thottathil, S. D., P. C. J. Reis, and Y. T. Prairie. 2019. Methane oxidation kinetics in northern freshwater lakes. Biogeochemistry **143**: 105–116. doi:10.1007/s10533-019-00552-x

Trolle, D., P. A. Staehr, T. A. Davidson, R. Bjerring, T. L. Lauridsen, M. Søndergaard, and E. Jeppesen. 2012. Seasonal dynamics of CO_2 flux across the surface of shallow temperate lakes. Ecosystems **15**: 336–347. doi:10.1007/s10021-011-9513-z

Vachon, D., and others. 2020. Paired O_2–CO_2 measurements provide emergent insights into aquatic ecosystem function. Limnol. Oceanogr.: Lett. **5**: 287–294. doi:10.1002/lol2.10135

Vanhellemont, Q. 2019. Adaptation of the dark spectrum fitting atmospheric correction for aquatic applications of

the Landsat and Sentinel-2 archives. Remote Sens. Environ. **225**: 175–192. doi:10.1016/j.rse.2019.03.010

Vera, M. S., and others. 2012. Direct and indirect effects of the glyphosate formulation Glifosato Atanor® on freshwater microbial communities. Ecotoxicology **21**: 1805–1816. doi:10.1007/s10646-012-0915-2

Viglizzo, E. F., F. Lértora, A. J. Pordomingo, J. N. Bernardos, Z. E. Roberto, and H. Del Valle. 2001. Ecological lessons and applications from one century of low external-input farming in the pampas of Argentina. Agric. Ecosyst. Environ. **83**: 65–81. doi:10.1016/S0167-8809(00)00155-9

Whiting, G. J., and J. P. Chanton. 2001. Greenhouse carbon balance of wetlands: Methane emission versus carbon sequestration. Tellus B Chem. Phys. Meteorol. **53**: 521–528. doi:10.3402/tellusb.v53i5.16628

Wickham, H. 2016. ggplot2: Elegant graphics for data analysis. Springer-Verlag.

Windham-Myers, L., B. Bergamaschi, F. Anderson, S. Knox, R. Miller, and R. Fujii. 2018. Potential for negative emissions of greenhouse gases (CO_2, CH_4 and N_2O) through coastal peatland re-establishment: Novel insights from high frequency flux data at meter and kilometer scales. Environ. Res. Lett. **13**: 045005. doi:10.1088/1748-9326/aaae74

Xiao, Q., and others. 2017. Spatial variations of methane emission in a large shallow eutrophic lake in subtropical climate. J. Geophys. Res.: Biogeo. **122**: 1597–1614. doi:10.1002/2017JG003805

Xing, Y., P. Xie, H. Yang, L. Ni, Y. Wang, and K. Rong. 2005. Methane and carbon dioxide fluxes from a shallow hypereutrophic subtropical lake in China. Atmos. Environ. **39**: 5532–5540. doi:10.1016/j.atmosenv.2005.06.010

Xing, Y., P. Xie, H. Yang, A. Wu, and L. Ni. 2006. The change of gaseous carbon fluxes following the switch of dominant producers from macrophytes to algae in a shallow subtropical lake of China. Atmos. Environ. **40**: 8034–8043. doi:10.1016/j.atmosenv.2006.05.033

Zimmer, K. D., W. O. Hobbs, L. M. Domine, B. R. Herwig, M. A. Hanson, and J. B. Cotner. 2016. Uniform carbon fluxes in shallow lakes in alternative stable states. Limnol. Oceanogr. **61**: 330–340. doi:10.1002/lno.10215

Zuur, A. F., E. N. Ieno, N. J. Walker, A. A. Saveliev, and G. M. Smith. 2009. Mixed effects models and extensions in ecology with R, v. **574**. Springer.

Acknowledgments

Conflict of Interest

None declared.